Identification of a macroscopic anisotropic damage model using digital image correlation and the equilibrium gap method

Laurent Crouzeix — Jean-Noël Périé — Francis Collombet Bernard Douchin

Université de Toulouse INSA, UPS, Mines Albi, ISAE; ICA (Institut Clément Ader) 133, avenue de Rangueil, F-31077 Toulouse

laurent.crouzeix@iut-tlse3.fr

ABSTRACT. *The aim of the work is to demonstrate how an anisotropic damage model may be identified from full field measurements retrieved during a heterogeneous test. The example of a biaxial test performed on a 3D C / C composite is used. In a first step, the displacement fields measured by classical Digital Image Correlation are used as input data of a finite difference version of the Equilibrium Gap Method. A benefit from unloadings (assumed to be elastic) is shown to retrieve a damage law. In a second step, inelastic strains can be assessed from the total measured strain and the elastic estimated strains. The constitutive parameters relative to the inelastic part of the model are then identified.*

RÉSUMÉ. *Le but du travail est de montrer comment un modèle d'endommagement anisotrope peut être identifié à partir de mesures de champs réalisées pendant un essai hétérogène. Un essai biaxial mené sur un composite 3D C/C sert d'exemple. On propose dans un premier temps d'utiliser les champs de déplacements mesurés par corrélation d'images numériques classiques en entrée d'une déclinaison différences finies de la méthode de l'ecart à l'équilibre (MEQ). L'utilisation de décharges (supposées élastiques) permet l'identification d'une loi d'endommagement. Dans un second temps, la déformation inélastique peut être estimée à partir de la déformation totale mesurée et de la déformation élastique estimée. Les paramètres constitutifs de la partie inélastique du modèle peuvent alors être identifiés.*

KEYWORDS: *identification*, *mechanical testing*, *anisotropic damage, inelasticity*, *full-field measurements.*

MOTS-CLES : *identification, essais mécaniques, endommagement anisotrope, inélasticité, mesures de champs.*

DOI:10.3166/EJCM.19.229-240

1. Introduction

The prediction of composite structures behaviour up to rupture is still a challenge. In this context, multi scale approaches that take into account the progressive failure are promising (Laurin *et al.*, 2007; Lubineau *et al.*, 2008). The identification of the numerous constitutive parameters introduced is based on a set of elementary tests. The specimens are usually neither representative of the application (e.g., multiaxial loadings) nor of the manufacturing process. The recent advances of full field measurements and simulation tools are opening the way for convenient and robust inverse methods exploiting heterogeneous tests.

Initiated by Sutton et al. (Sutton *et al.*, 1983), Digital Image Correlation (DIC) is now a widely spread full field measurement technique. It offers a simple and unique opportunity to assess displacement fields on various scales, but also in the bulk (Bay, 1999). It is here proposed to exploit DIC displacement fields measured on the surface of a cross-shaped specimen during a biaxial test (Périé *et al.*, 2002) in order to identify a macroscopic anisotropic damage model.

Many identification methods have yet been proposed to exploit the heterogeneity of measured kinematical fields (Avril *et al.*, 2008). Among those, the Finite Element Model Updating method (FEMU) (Molimard *et al.*, 2005) (Le Magorou *et al.*, 2002) or the Virtual Fields Method (VFM) (Pierron *et al.*, 2007) have mostly been used to retrieve orthotropic elastic parameters from inhomogeneous experiments, but also to study damage (Chalal *et al.*, 2004) (Geers *et al.*, 1999) or plasticity (Cooreman *et al.*, 2007). The aim of this paper is to show how the Equilibrium Gap Method can help to identify both a damage law and inelastic parameters involved in an anisotropic damage model.

In the following section, one quickly describes the studied material (a 3D Carbon/Carbon composite) and the associated macroscopic model (including anisotropic damage and inelasticity). The experimental setup of the biaxial shear test performed on a cruciform specimen is also presented. In the third section, the basic principal of the EGM is briefly stated. A finite difference version dealing with orthotropic materials is commented. In the fourth section, it is first shown how, from a set of displacement fields and a given damage mechanism, the method may lead to assess a damage growth law and damage maps relative to the shear modulus. In a second step, it is then proposed to extract the inelastic shear strain field and to compute the shear stress field in order to complete the model identification.

2. Material, modelling and experimental setup

2.1. *Material and modelling*

The material is obtained by stacking and needling plies of satin layers made of carbon yarn. The matrix is synthesized in the preform by a Chemical Vapour

Infiltration (CVI) technique. For the studied $[0,90]_n$ laminate, tensile tests reveal an anisotropic behaviour with damage (*i.e.* failing in rigidity) and inelastic strains (*i.e.* permanent strains) at 45° but also at 0°.

As the laminate thickness is negligible compared with other dimensions (typically 10 mm versus more than 100 mm), a state of plane stress is assumed and the classical laminate theory is used. *(1, 2)* indices refer to the ply coordinate system here coinciding with the fibre direction. With these notations, E_1 and E_2 denote the initial Young's moduli (here in the fibre directions), G_{12} the initial shear modulus and υ_{12} Poisson's ratio. The angle between this frame and that of the reference coordinate system *(x, y)* is θ.

The damage model considered here (Hochard *et al.*, 2007) is derived from an approach originally introduced for unidirectional plies (Ladevèze *et al.*, 1992). Three damage variables are used. As the first step, the damage variables d_1 and d_2 account for the brittle fracture in the fibre direction. The parameter d_{12} describes a gradual degradation of the shear modulus. This behaviour is representative of many [0, 90] carbon / epoxy woven composites. A continuum thermodynamics framework is used. Gibbs' free energy density ψ of the woven ply reads [1].

$$\psi = \frac{1}{2}\left(\frac{\langle \sigma_{11} \rangle_+^2}{E_1(1-d_1)} + \frac{\langle \sigma_{11} \rangle_-^2}{E_1} + \frac{\langle \sigma_{22} \rangle_+^2}{E_2(1-d_2)} + \frac{\langle \sigma_{22} \rangle_-^2}{E_2} - 2\frac{\nu_{12}}{E_1}\sigma_{11}\sigma_{22} + \frac{{\sigma_{12}}^2}{G_{12}(1-d_{12})} \right) \quad [1]$$

The positive parts σ_{ij}^+ of the stress σ_{ij} is useful to model deactivation of the damage due to crack closure, depending on the sign of the applied stress. State laws can be derived from the state potential ψ. For each damage variable d_i, a driving force Y_{di} could be written [2].

$$Y_{d_i} = \frac{\partial \Psi}{\partial d_i} = \frac{1}{2}\frac{\langle \sigma_{ii} \rangle_+^2}{E_i(1-d_i)^2} \text{ for } i = 1 \text{ or } 2, \text{ and } Y_{d_{12}} = \frac{\partial \Psi}{\partial d_{12}} = \frac{1}{2}\frac{{\sigma_{12}}^2}{G_{12}(1-d_{12})^2} \quad [2]$$

In the present case, the growth of d_{12} is assumed to be only related to its associated driving force Y_{d12}. The following notations are used in the sequel as $d = d_{12}$ and $Y = Y_{d12}$. One defines an equivalent strain ε_{eq} [3]:

$$\left|\varepsilon_{eq}\right| = \sqrt{\frac{Y}{2G_{12}}} = \left|\varepsilon_{12}\right| = \frac{1}{2}\left|\left(\varepsilon_{yy} - \varepsilon_{xx}\right)\sin 2\theta + 2.\varepsilon_{xy}\cos 2\theta\right| \quad [3]$$

In the present case ($\theta \approx 45°$), the equivalent strain is the absolute value of the elastic shear strain expressed in the ply coordinate system.

Inelastic strains are assumed to be generated by friction and non-closure of cracks in the matrix. They are here described by a plasticity model with isotropic hardening. It is here assumed that only shear inelastic strains may appear (the fibres prevent from tensile inelastic strains). The coupling between inelastic strains and

damage is then accounted in terms of the effective stress and the effective strain [4] (Ladevèze *et al.*, 1992).

$$\tilde{\sigma}_{12} = \frac{\sigma_{12}}{1 - d_{12}} \text{ and } \dot{\tilde{\varepsilon}}_{12}^{\,p} = \dot{\varepsilon}_{12}^{\,p}\left(1 - d_{12}\right) \quad [4]$$

It is here assumed that the stresses σ_{11} and σ_{22} do not influence the yield surface defined by [5].

$$f\left(\tilde{\sigma}, p\right) = \left|\tilde{\sigma}_{12}\right| - \left(R_0 + R(p)\right) \leq 0 \quad [5]$$

where R_0 represents the initial threshold for the inelastic strain and $R(p)$ is the hardening function of the accumulated inelastic strain p.

The function $R(p)$ is chosen such as [6].

$$R\left(p\right) = \beta . p^{\gamma} \quad [6]$$

The plastic flow is given by [7]

$$\dot{\tilde{\varepsilon}}_{12}^{\,p} = \dot{p}\,\frac{\partial f}{\partial \tilde{\sigma}_{12}} = \dot{p}\,\frac{\tilde{\sigma}_{12}}{R_0 + R(p)} \text{ with } \dot{p} = \left|\dot{\tilde{\varepsilon}}_{12}^{\,p}\right| \quad [7]$$

where $\dot{p}$ represents the rate of cumulative plastic strain.

2.2. *Biaxial test*

The experiment treated herein consists in a biaxial test performed on a 3D C/C composite (Périé, 2002). The test has been carried out on the multiaxial machine ASTREE located in the LMT-Cachan (France). A flat (10 mm thick) cruciform specimen is subjected to a shear test (see Figure 1). Tabs glued on the arms (100 mm large) allow for a transmission of the loads to the specimen (see Figure 1c). This test was designed, in particular thanks to FE computations, to induce a high value of shear damage in the center part of the specimen. A scheme of the loading path is proposed in Figure 1b.

Digital images of the surface (1016 × 1008 pixels, 8-bit digitization) shot at various steps of the loading (see Figure 1b) are analysed using a DIC procedure (Hild *et al.*, 2002). The ZOI (Zone Of Interest) size S, chosen according to the speckle pattern of the specimen, is equal to 64 pixels. The shift p between two ZOIs is set to 32 pixels (*i.e.*, ca. 3 mm). The image resolution (or magnification), g is 0.047 μm/pixel. The spatial resolution is then S*g = 3 mm.

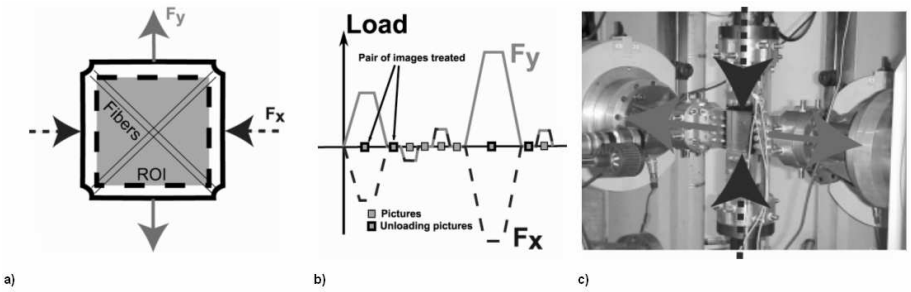

Figure 1. *Biaxial test on a cruciform specimen made of a 3D C/C composite with: a) Principle of the experiment b) Loading path c) Experimental setup*

3. A finite difference version of the EGM for orthotropic materials

The EGM consists in looking for contrasts of mechanical properties that lead "at best", for the given (measured) displacement field, to the internal equilibrium (in the bulk). In the pioneer work presented in (Claire *et al.*, 2002), the authors resort to a FE approach to describe the equilibrium. For elastic isotropic behaviour, this weak form of the EGM leads to a linear system, where the unknowns are the contrasts between element wise constant Young's moduli, and the input data are the displacements measured at the nodes. A reconditioned FE version of the EGM has recently been used to study orthotropic materials (Périé *et al.*, 2009).

An alternative finite difference scheme has been proposed in (Crouzeix *et al.*, 2009). The equilibrium is then directly expressed in terms of resultants instead of a minimisation of the strain energy. This choice is consistent with the way information are assessed and treated in usual DIC softwares. In addition, this numerical scheme leads to a simple implementation and physical meaning of the method.

The solid is split in cells. The cell borders are constructed on the regular DIC grid. In each cell, the behaviour is assumed to be elastic, homogeneous and orthotropic. The material orthotropy axes are identical in all the cells. As suggested in (Claire *et al.*, 2002), the equilibrium between adjacent cells is first considered. It leads to write the continuity of the normal stress vector across the interface $\partial\omega$ between two adjacent cells [8].

$$\left[\boldsymbol{\sigma}\underline{n}\right] = \underline{0} \text{ on } \partial\omega \qquad [8]$$

where $[\underline{x}]$ denotes the jump of $\underline{x}$ and $\underline{n}$ the normal to $\partial\omega$.

The stresses in each cell are simply computed from the estimated strains (central differences) and unknown rigidities. One then obtains relationships between measured displacements and rigidities of two adjacent cells. For each interface, two scalar equations can be written. They are both linear with respect to the rigidities of

the cells. For an inner cell, this would lead to 8 equations. Nevertheless, one has to note that the numbers of unknowns have increased with respect to the isotropic case. Additional equations are then formed by writing the equilibrium of inner cells and of inner corner nodes. One may refer to the work presented in (Crouzeix *et al.*, 2009) for additional details.

Because the equations simply link the material properties of adjacent cells through the measured displacements, the EGM only gives access to the contrast $\delta_{p(i,j)}$ of the property $K_{p(i,j)}$ in cell *(i,j)* with respect to an arbitrary reference modulus K_{po} [9].

$$K_{p_{(i,j)}} = K_{p_o}(1-\delta_{p_{(i,j)}}) \qquad [9]$$

An overdetermined (typically by a factor of 1.8 for a grid of 20 x 20 cells) system of linear equations is finally formed. It is solved by using a conjugate gradient method (a preconditioning matrix transforms the system into a square form). When static quantities are known, namely, resultants or moments on the boundaries of the Region Of Interest (ROI), one may then use a one-step finite element updating method in order to find the reference modulus K_{po}. In the following, such data are not available. A specific procedure, inspired by (Claire *et al.*, 2007), is followed.

4. Identification procedure

The DIC procedure gives a displacement fields with respect to a given reference state. When using the first image as the reference, the measured displacement fields result not only from damage but also from inelasticity. We propose here a two-step procedure. In a first step, one then elects to identify the damage law relating the shear damage variable d to the equivalent strain ε_{eq}. We then use the EGM with displacement fields corresponding to unloading/loading cycles. In a second step, one can evaluate the inelastic deformation in any cell and at any stage of the loading. One can finally identify the parameters of the modelling relative to the inelastic behaviour (R_0, p, γ).

4.1. *From contrast fields to damage fields*

The 11 unloading/loading cycles are used to assess only the change of rigidity $G_{12} = G_0 (1-d_{12})$. The hysteretic (inelastic) effects are then ignored and the unloading is considered purely elastic. Here 11 pairs of pictures are used (see Figure 1b). The first picture is taken at the maximum load level of a given cycle, and the second one at the subsequent unloaded state (in terms of load in each arm).

A contrast map may be plotted for each of the four rigidities at each loading level. The effect of noise is perceptible for the first two levels due to the low

amplitude of the displacements; however, some characteristic patterns already appear at the 3rd step and are present until fracture. Here, the first two maps are not used. As expected, a lower rigidity in the centre of the specimen is observed. The contrast between the centre and the edges of the ROI is noted to increase with the loading level.

In the present case, due to the test configuration, the ROI is not large enough to intercept the loading arms. Consequently, it is not possible to retrieve directly the value of the mean shear modulus. The initial modulus G_{12}^0 can be assessed accurately from tensile tests performed on the same material (G_{12}^0=9.9 GPa). Nevertheless, one may note that the non linear part of the stress-strain curves retrieved for this material using tensile tests and various strain gages are very scattered. They are consequently unusable for the identification of non linear parameters.

An alternative route is then followed. One may note that the procedure has been validated using simulated data (Crouzeix *et al.*, 2009) (the effect of noise has also been addressed). The identified contrasts of moduli δ_{12} are assumed to result from a unique damage growth law. In each cell $\omega_{i,j}$, the equivalent strain ε_{eq} is computed from the measured displacement field. Figure 2a shows the distribution for each identified map of $log(1-\delta_{12})$ versus $log(\varepsilon_{eq})$ for each successive load level. All the obtained point clouds are well fitted by straight lines. The position of these clouds depends on the reference chosen for each map. These results show that the damage law can be described using a simple power law. The reference modulus for each loading stage is then adjusted to collapse all the contrast data onto a unique curve $d(\varepsilon_{eq})$ as shown in Figure 2b.

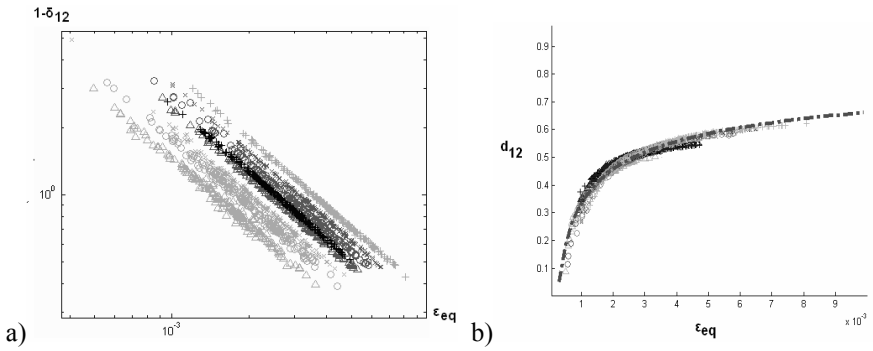

Figure 2. *a) Identified local contrasts ($1-\delta_{12}$) with respect to its associated equivalent strain ε_{eq} for each unloading/loading cycle. b) Evolution of the local damage d_{12} with respect to ε_{eq}*

Figure 3 shows some identified damage maps corresponding to the last loading stages. As expected, a progressive increase of the damage level is noted, and more specifically, in the centre of the ROI. The maximum value of the damage reached in

this region is around 0.55. In (Perie *et al.*, 2002), the material was considered as a [±45°] laminate. For each ply direction, the same damage mesomodel was proposed. The damage field inside each layer within the ROI was computed by using a damage post-processor. One notes a good agreement between these post-processed damage maps and that determined by following the present procedure (Crouzeix *et al.*, 2009).

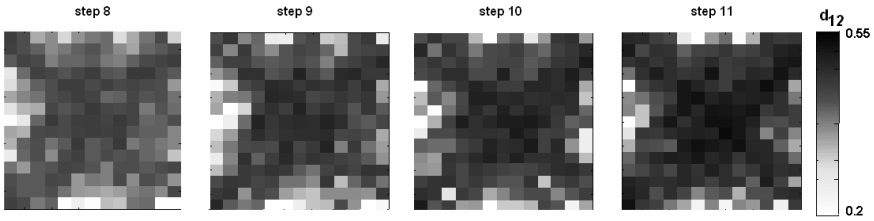

Figure 3. *Identified damage maps for the 5 last loading steps*

4.2. *Inelastic behaviour*

Given the damage law, it is now proposed to identify the inelastic behaviour. On the one hand, the shear stress field can be evaluated just before an unloading. It may be computed using the measured shear elastic strain ε_{12}^{el} field (estimated from the unloading/loading cycle) and the damage d_{12} field previously identified [10].

$$\sigma_{12} = G_{12}^{0}(1-d_{12})\varepsilon_{12}^{el} \qquad [10]$$

The corresponding effective stress field (see [4]) simply reads [11].

$$\tilde{\sigma}_{12} = G_{12}^{0}\varepsilon_{12}^{el} \qquad [11]$$

The loading surface radius $R+R_0$ can then be estimated from the equation [12].

$$R^{(i)} + R_0 = \sqrt{2\int_0^{\sigma_{12}^{\max(i)}} \frac{\sigma_{12}}{\left(1-d_{12}^{(i)}\right)^2} d\sigma_{12}} = \sqrt{2\int_0^{\sigma_{12}^{\max(i)}} \frac{\tilde{\sigma}_{12}}{\left(1-d_{12}^{(i)}\right)} d\sigma_{12}} \qquad [12]$$

At this stage, the evolution of $\tilde{\sigma}_{12} \Big/ 1-d_{12}^{(i)}$ with respect to σ_{12} can be plotted in each cell (see Figure 4) for the different unloadings considered. In practice, for each loading step i (*i.e.* for cell of each image), $R^{(i)}+R_0$ is evaluated by computing the area under the interpolated (quadratic polynomial) curve plotted in Figure 4 (the correlation coefficient R is here 0.985) .

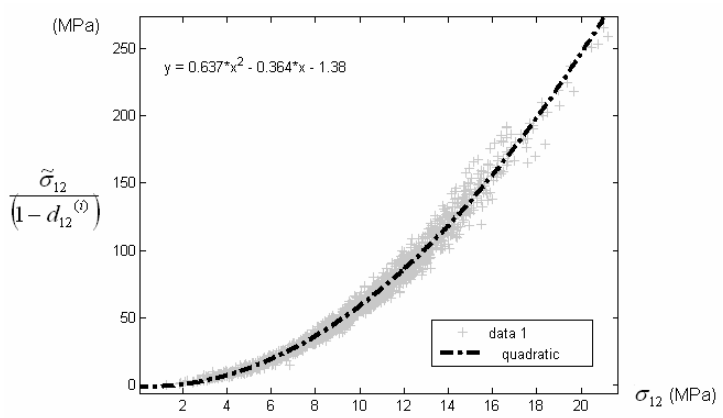

Figure 4. C*omputation of the loading surface radius: experimental points (circles), and fitted curve (in dotted line)*

On the other hand, one can evaluate the inelastic shear strain in each cell. The total shear strain field (ε_{12}) can indeed be measured using the first image (initial unloaded state) and the image shot just before unloading the specimen. A simple difference between this field and the elastic one (ε_{12}^{el}) gives access to the inelastic shear strain field ($\varepsilon_{12}^{p} = \varepsilon_{12} - \varepsilon_{12}^{el}$) before each unloading. One can here simply compute the cumulated plastic strains p using [7]. The master curve relative to the isotropic hardening can finally be plotted (see Figure 5). The best fit is obtained for the following constitutive parameters: $R_0 = 6.1$ MPa, $\beta = 2240$ MPa, $\gamma = 0.66$.

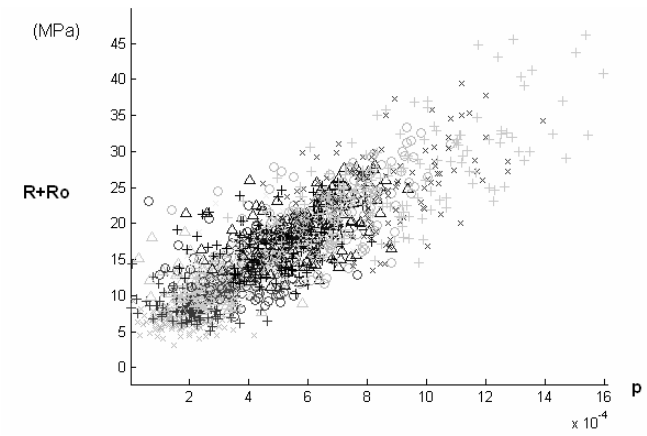

Figure 5. *Identification of the plasticity model with isotropic hardening*

The result is scattered. On the one hand, this observation may be linked to the relative magnitude of the strain uncertainties (estimated to be of the order of a few 10^{-4}) with respect to the measured inelastic strains. It has been shown in (Crouzeix *et al,* 2009) the low influence of the noise in the identification procedure. We notice that the obtained noise (Figure 5.) is mainly the effect of strain uncertainties along the horizontal axis. On the other hand, the isotropic hardening assumption is probably too rough to describe the real evolution of shear strains in such material. Kinematic hardening should certainly also be considered.

5. Conclusion

An identification procedure of an anisotropic damage behaviour based on full field measurements is proposed. It is applied to analyse a biaxial shear test previously performed on a C/C composite. For such an experiment, it can be shown that important shear damage takes place in the centre part of the specimen.

In the second section, the tested material and the associated modelling are first presented. The proposed model, based on a continuum damage approach (CDM), is recalled. In the present case, as a first approximation, shear damage simply depends on an equivalent strain, directly related to the measurements. A plasticity model with isotropic hardening is used to describe the evolution of inelastic strains during the experiment. A coupling between damage and plasticity is introduced. The experimental setup of the biaxial test is finally presented.

In the third section, an orthotropic variant of the EGM is briefly presented. This finite difference version is consistent with information given by classical DIC softwares. The solid is then divided into cells, whose boundaries coincide with the measurement grid. The technique consists in solving a linear system for which the known data are measured displacements, and the unknowns are the rigidity contrast fields.

In the last section, a two-step procedure is proposed to identify the constitutive parameters of the chosen macroscopic model. In a first step, a damage law is identified. In practice, contrast maps are first retrieved by using the proposed EGM procedure. These maps are then assumed to result from a single damage law. In a second step, one identifies the parameters of the plasticity model. The idea is then to compute shear stress fields and inelastic shear strains fields at the beginning of the various unloadings.

The advantage of the present version of the EGM is that it permits the study of (heterogeneous) composite structures or heterogeneous composite materials (Marguerès *et al.*, 2009). The macroscopic behaviour of distinct zones of technological specimens (e.g., filament wound pipe (Hernandez-Moreno *et al.*, 2008), in particular, could be addressed. Current zones (e.g., laminated regions) could be initially considered as *homogeneous* to limit the effect of the measurement uncertainty. On the

contrary, the behaviour in cells included in singular regions (e.g., woven regions) could be left freer in order to propose a relevant macroscopic modelling.

6. References

Avril S., Bonnet M., Bretelle A.-S., Grédiac M., Hild F., Ienny P., Latourte F., Lemosse D., Pagano S., Pagnacco E., Pierron F., "Identification from measurements of mechanical fields", *Exp. Mech.*, vol. 48, n° 5, 2008, p. 381-402.

Bay B., Smith T., Fyhrie D., Saad M., "Digital volume correlation: three-dimensional strain mapping using x-ray tomography", *Exp.Mech.*, vol. 39, n° 3, 1999, p. 217-226.

Chalal H., Meraghni F., Pierron F., Grédiac M., "Direct identification of the damage behaviour of composite materials using the virtual fields method", *Composites Part A*, vol. 35, n° 7-8, 2004, p. 841-848.

Claire D., Hild F., Roux S., "Identification of damage fields using kinematic measurements", *C. R. Mécanique*, 2002, 330, p. 729-734.

Claire D., Hild F., Roux S., "Identification of a damage law by using full-field displacement measurements", *Int. J. Damage Mech.*, vol. 16, 2007, p. 179-197.

Cooreman S., Lecompte D., Sol H., Vantomme J., Debruyne D., "Elasto-plastic material parameter identification by inverse methods: Calculation of the sensitivity matrix", *International Journal of Solids and Structures*, vol. 44, n° 13, 2007, p. 4329-4341.

Crouzeix L., Périé J.-N., Collombet F., Douchin B., "An orthotropic variant of the equilibrium gap method applied to the analysis of a biaxial test on a composite material", *Composite: Part A*, vol. 40, 2009, p. 1732-1740.

Geers M. G. D., de Borst R., Peijs T., "Mixed numerical-experimental identification of non-local characteristics of random-fibre-reinforced composites", *Comp. Sci. Tech.*, vol. 59, n° 10, 1999, p. 1569-1578.

Hernandez Moreno H., Douchin B., Collombet F., Davies P., Choqueuse D., "Influence of winding pattern on the mechanical behavior of filament wound composite cylinders under external pressure", *Composites Science and Technology*, vol. 68, n° 3-4, 2008, p. 1015-1024.

Hild F., Raka B., Baudequin M., Roux S., Cantelaube F., "Multiscale displacement field measurements of compressed mineral-wool samples by digital image correlation", *Appl Opt*, vol. 41, n° 32, 2002, p. 6815-6828.

Hochard C., Lahellec N., Bordreuil C., "A ply scale non-local fibre rupture criterion for CFRP woven ply laminated structures", *Comp. Struct.*, vol. 80, n° 3, 2007, p. 321-326.

Ladevèze P., LeDantec E., "Damage modelling of the elementary ply for laminated composites", *Comp. Sci. Tech.*, vol. 43, 1992, p. 257-267.

Laurin F., Carrère N., Maire J.F., "A multiscale progressive failure approach for composite laminates based on thermodynamical viscoelastic and damage models", *Composites Part A*, vol. 38, n° 1, 2007, p. 198-209.

Lubineau G., Ladevèze P., "Construction of a micromechanics-based intralaminar mesomodel, and illustrations in ABAQUS/Standard", *Computational Materials Science*, vol. 43, n° 1, 2008, p. 137-145.

Marguerès P., Périé J.-N., Perez J. G., Collombet F., Grunevald Y., "Characterization of a composite structure obtained by RFI using HexFIT® semi-products", *Composites Science and Technology*, vol. 69, n° 1, 2009, p. 117-124.

Molimard J., Le Riche R., Vautrin A., Lee J.-R., "Identification of the four orthotropic plate stiffnesses using a single open-hole tensile test", *Exp.Mech.*, vol. 45, n° 5, 2005, p. 404-411.

Périé J.-N., Calloch S., Cluzel C., Hild F., "Analysis of a multiaxial test on a C/C composite by using digital image correlation and a damage model", *Exp. Mech.*, vol. 42, n° 3, 2002, p. 318-328.

Périé J.-N., Leclerc H., Roux S., Hild F., "Digital image correlation and biaxial test on composite material for anisotropic damage law identification", *International Journal of Solids and Structures*, vol. 46, n° 11-12, 2009, p. 2388-2396.

Pierron F., Vert G., Burguete R., Avril S., Rotinat R., Wisnom M.-R., "Identification of the orthotropic elastic stiffnesses of composites with the virtual fields method: sensitivity study and experimental validation", *Strain*, vol. 43, n° 3, 2007, p. 250-259.

Sutton M. A., Wolters W. J., Peters W. H., Ranson W. F., McNeill S. R., "Determination of displacements using an improved digital correlation method", *Image Vision and Computing*, vol. 1, n° 3, 1983, p. 133-139.